

Electronic Supplementary information

Plasmonic-enhanced carbon dots based semi-transparent Luminescent Solar Concentrator

Xin Liu^a, Daniele Benetti^{a,*} Federico Rosei^{a, **}

^a Centre for Energy, Materials and Telecommunications, Institut National de la Recherche Scientifique, 1650 Boulevard Lionel-Boulet, Varennes, Québec J3X 1S2, Canada.

* Corresponding author. Tel.: 1-514-2286995. E-mail address: daniele.benetti@inrs.ca

**Corresponding author. Tel.: +1-514-2286906; E-mail address: federico.rosei@inrs.ca

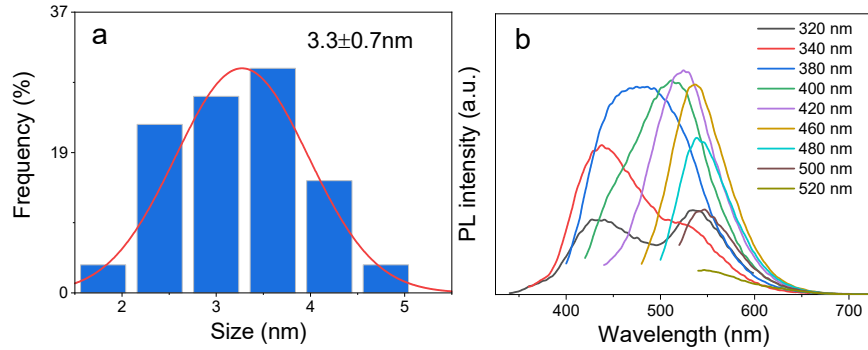


Fig S1. (a) Size distribution of as-prepared Cdots, (b) PL spectra of Cdots at different excitation wavelengths

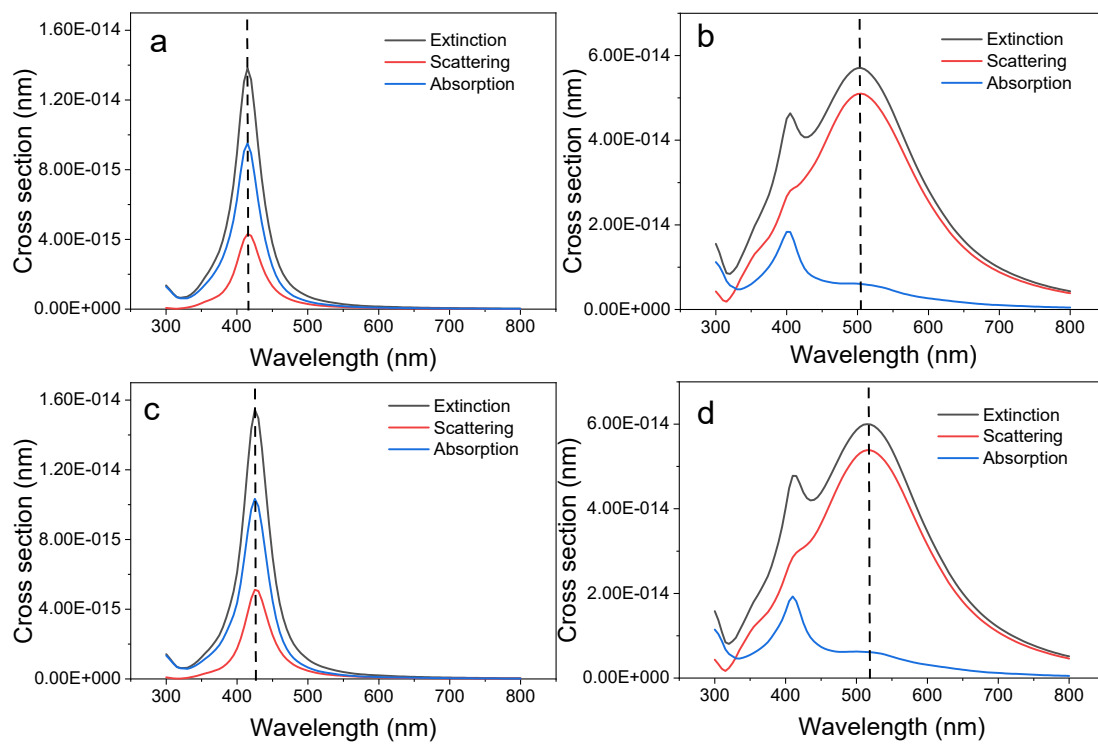


Fig S2*. Simulated extinction, scattering, and absorbance spectra for Ag NPs: (a) Ag40, (b) Ag100, (c) Ag40@10nmSiO₂, (d) Ag100@10nmSiO₂. (* Data is from the open resources in nanocomposix.com)

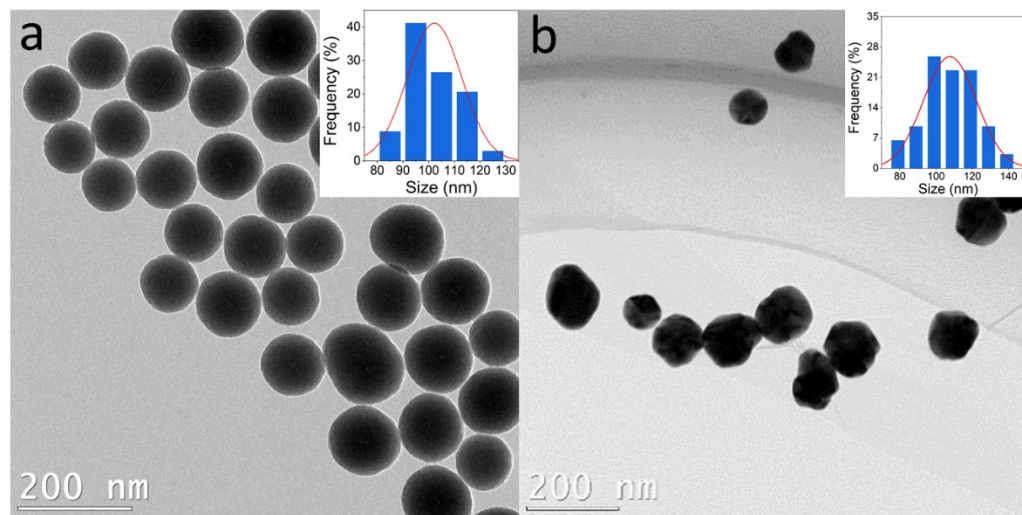


Fig S3. TEM image of as-prepared scattering NPs: (a) SiO_2 , (b) Ag100 NPs, the inset figures are the size distribution of the samples

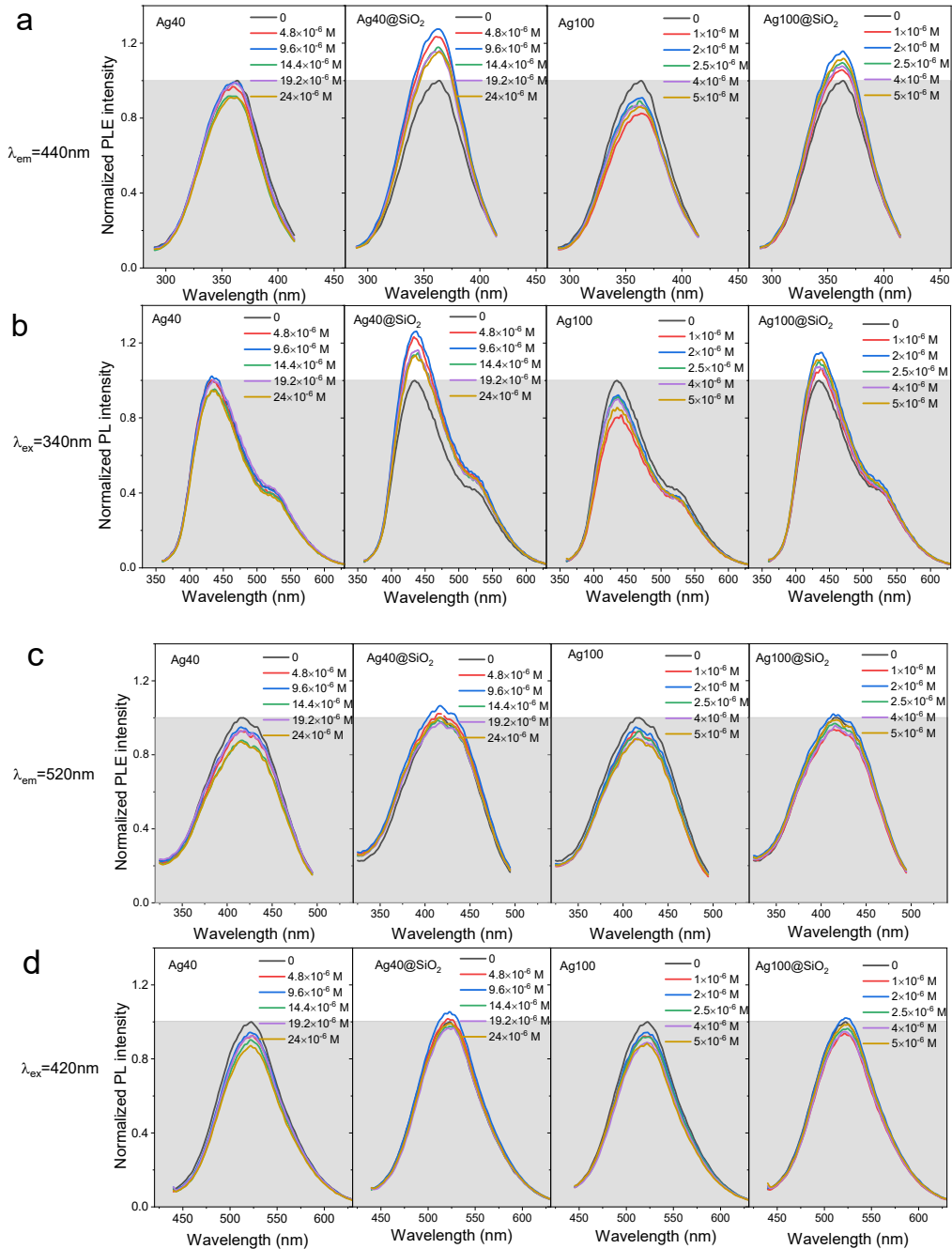


Fig S4. PL excitation and PL emission spectra of Cdots (0.1mg/ml) with Ag and Ag@SiO₂ at different concentrations measured in ethanol, (a) PL excitation spectra obtained at emission wavelength of 440nm, (b) PL emission excited at 340nm, (c) PL excitation spectra obtained at emission wavelength of 520nm, (d) PL emission excited at 420nm.

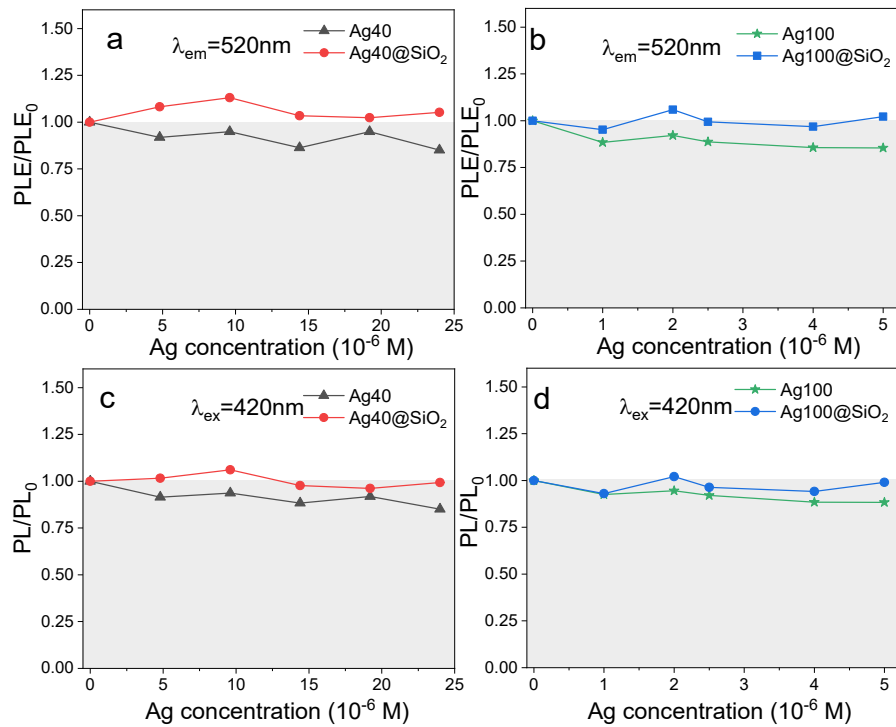


Fig S5. PL excitation and PL emission relative changes of Cdots (0.1mg/ml) with Ag and Ag@SiO₂ at different concentrations measured in ethanol, (a)(b) plotted PL excitation integrals obtained at emission wavelength of 520nm, (c) (d) plotted PL emission integrals excited at 420nm. PLE₀ was PL excitation peak integrals of bare Cdots and PLE is PL excitation integrals of Cdots with plasmonic NPs, PL₀ was emission peak integrals of bare Cdots and PL is emission integrals of Cdots with plasmonic NPs.

Table S1. PL decay parameters of Cdots and Cdots-Ag@SiO₂

Samples	A ₁	τ _{1/ns}	A ₂	τ _{2/ns}	τ _{ave/ns}
Cdots	0.08	3.01	0.92	10.42	9.62
Cdots-Ag@SiO ₂	0.07	2.45	0.93	10.74	9.92

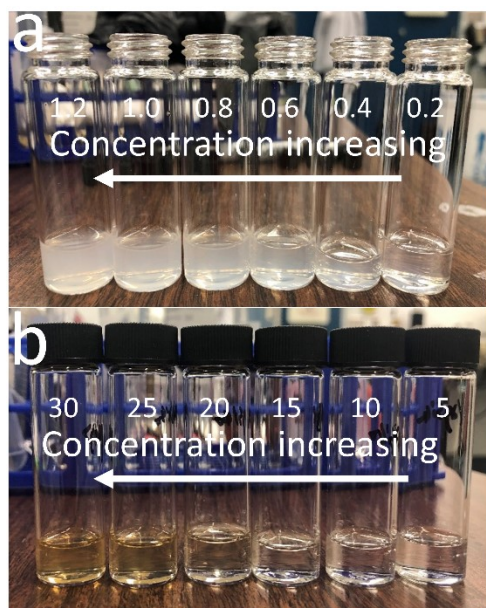


Fig S6. Silver NPs dispersed in ethanol at different concentrations: (a) SiO₂ ($\times 10^{-3}$ M), (b) Ag40@SiO₂ ($\times 10^{-6}$ M)



Fig S7. Liquid LSC fabricated with quartz cells: (a) Bare Cdots, (b) Cdots + Ag40@SiO₂, (c) Cdots + SiO₂

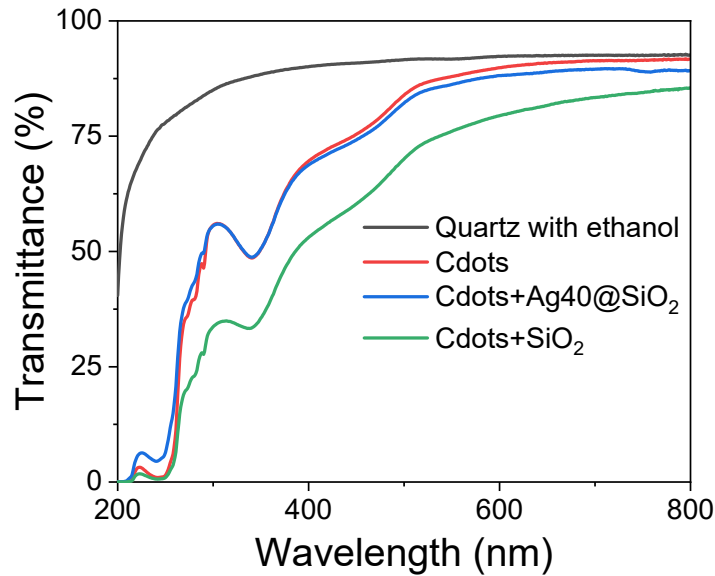


Fig S8. Transmittance of liquid LSCs with different luminophores in quartz cells. The concentration of Cdots, Ag40@SiO₂ and SiO₂ are: 0.1mg/ml, 9.6×10^{-6} M and 1.2×10^{-3} M respectively.

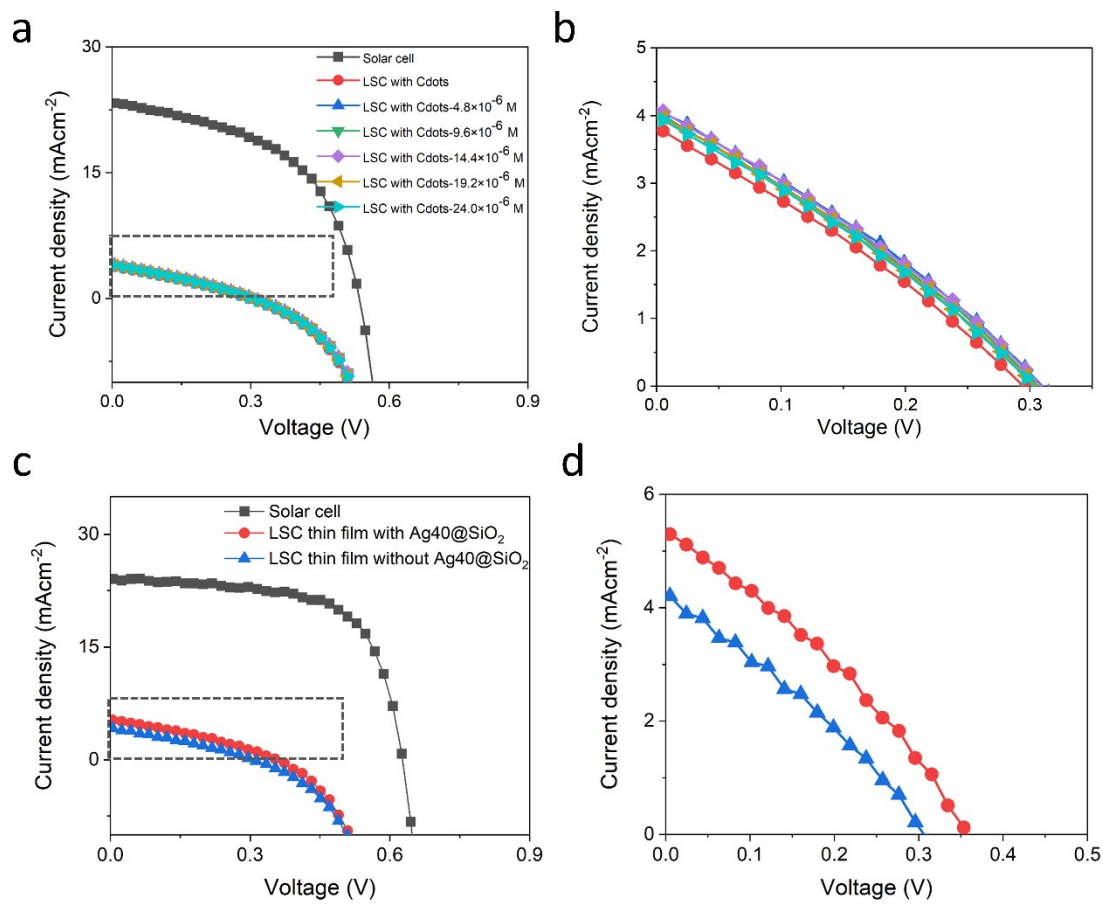


Fig.S9 J-V curves of Silicon solar cells with and without LSCs: (a) $G = 15$, (b) zoom of dashed area in (a); (c) $G = 25$; (d) zoom of dashed d area in (c)

Table S2. Photovoltaic parameters of Si solar cell coupled with Cdots-Ag40@SiO₂ based

Samples	J _{sc} /mA cm ⁻²	V _{oc} /V	FF	PCE/%	$\eta_{opt}/\%$
Si Solar cell	23.42	0.53	0.51	6.33	-
Cdots	3.75	0.29	0.29	0.31	1.05
Cdots- $4.8 \times 10^{-6} M$ Ag40@SiO ₂	4.25	0.31	0.30	0.40	1.20
Cdots- $9.6 \times 10^{-6} M$ Ag40@SiO ₂	4.35	0.32	0.31	0.43	1.23
Cdots- $14.4 \times 10^{-6} M$ Ag40@SiO ₂	4.14	0.31	0.29	0.37	1.17
Cdots- $19.2 \times 10^{-6} M$ Ag40@SiO ₂	3.98	0.30	0.29	0.35	1.13
Cdots- $24.0 \times 10^{-6} M$ Ag40@SiO ₂	4.00	0.29	0.29	0.34	1.13

liquid LSCs (G=15)**Table S3. Photovoltaic parameters of Si solar cell coupled with Cdots based thin film LSCs at different edges (1#, 2# and 3#) (G=25)**

Samples	No.	J _{sc} /mA cm ⁻²	V _{oc} /V	FF	PCE/%	$\eta_{opt}/\%$
Si Solar cell	-	24.07	0.63	0.64	9.70	-
	1#	4.22	0.31	0.31	0.41	0.71
Cdots	2#	4.23	0.31	0.31	0.40	0.72
	3#	3.83	0.29	0.30	0.38	0.65
Cdots-	1#	4.58	0.33	0.31	0.47	0.78
Ag40@SiO ₂	2#	4.99	0.34	0.32	0.55	0.85
	3#	5.97	0.36	0.32	0.62	0.90

Table S4. Power conversion efficiency of the LSC, η_{LSC} , calculated for Cdots-Ag40@SiO₂

Samples	J _{sc} /mA cm ⁻²	V _{oc} /V	FF	$\eta_{LSC}/\%$
Cdots	0.38	0.29	0.29	0.13
Cdots- $4.8 \times 10^{-6} M$ Ag40@SiO ₂	0.43	0.31	0.30	0.16
Cdots- $9.6 \times 10^{-6} M$ Ag40@SiO ₂	0.44	0.32	0.31	0.17
Cdots- $14.4 \times 10^{-6} M$ Ag40@SiO ₂	0.41	0.31	0.29	0.15
Cdots- $19.2 \times 10^{-6} M$ Ag40@SiO ₂	0.40	0.30	0.29	0.14
Cdots- $24.0 \times 10^{-6} M$ Ag40@SiO ₂	0.40	0.29	0.29	0.13

based liquid LSCs (G=15).

Samples	$\eta_{LSC}/\%$	$\eta_{LSC}^*/\%$
Cdots	0.13	0.23
Cdots- $4.8 \times 10^{-6} M$ Ag40@SiO ₂	0.16	0.26
Cdots- $9.6 \times 10^{-6} M$ Ag40@SiO ₂	0.17	0.27
Cdots- $14.4 \times 10^{-6} M$ Ag40@SiO ₂	0.15	0.25

Cdots- $19.2 \times 10^{-6} M$ Ag40@SiO ₂	0.14	0.24
Cdots- $24.0 \times 10^{-6} M$ Ag40@SiO ₂	0.13	0.24

Table S5. Liquid LSC power conversion efficiencies obtained with direct and indirect estimation.

The indirect estimation of η_{LSC}^* is obtained accordingly to the formula: $\eta_{LSC}^* = \eta_{PV}^* \times \eta_{opt}^1$, where η_{PV}^* is the PV efficiency under PL spectra and intensity of luminophores, and η_{opt}^* is the overall optical efficiency.

Due to the complicated derivations of η_{PV}^* that introduces some overestimation, and the optical efficiency data obtained from the formula of the mirror configuration, the obtained η_{LSC}^* present higher values. However, we can observe that the two η_{LSC} values calculated with the two formulae follow a very similar trend, confirming the beneficial effect of the presence of plasmonic Ag nanoparticles.

Table S6. Comparison of the experimental parameters of plasmonic metal NPs introduced LSCs

Fluorophore	Plasmonic particles	QY(%)	LSC size(cm ³)	Waveguides	G	Efficiency (%)	Refs
Carbon dots	Ag@SiO ₂ NPs	~30%	2.0 × 2.0 × 0.2	Liquid LSC	15	+25% improvement (OE=1.23)	This work
Carbon dots	Ag@SiO ₂ NPs	~30%	5.0 × 5.0 × 0.2	PVP thin film	25	+25% improvement (OE=0.90)	This work
CdSe/ZnS QDs	Au NPs	-	1 cm cuvette	PMMA	-	LSC not realized	²
<i>CdSe/ZnS</i>						No Optical	

Efficiency was reported.							
Tetraphenyl porphyrin (TPP) Coumarin 6	Ag@SiO ₂ NPs	-	2.2 × 2.2 × 0.2	Layer-by-layer thin film	2.75	OE= 1.34 – 1.84	⁴
Red305	Au@Ag nanocuboids	~100%	4.5×4.5×0.3	DOWSIL EI1184	-	1.2 times PCE enhancement	⁵
L-glutathione	Au nanoclusters	25%	-	PVP thin film	-	OE=1.85	⁶
Yellow 10 GN+Red G	Au NPs, Ag NPs	87%, 86.5%	2.5 × 2.5×0.1	PMMA Tandem	-	Tandem system PCE increased from 6.12 to 10.37 with NPs	⁷
DCJTB (C ₃₀ H ₃₅ N ₃ O)	Ag NPs	-	-	PMMA	-	PCE=1.84-1.96	⁸

OE=optical efficiency, PCE=power conversion efficiency

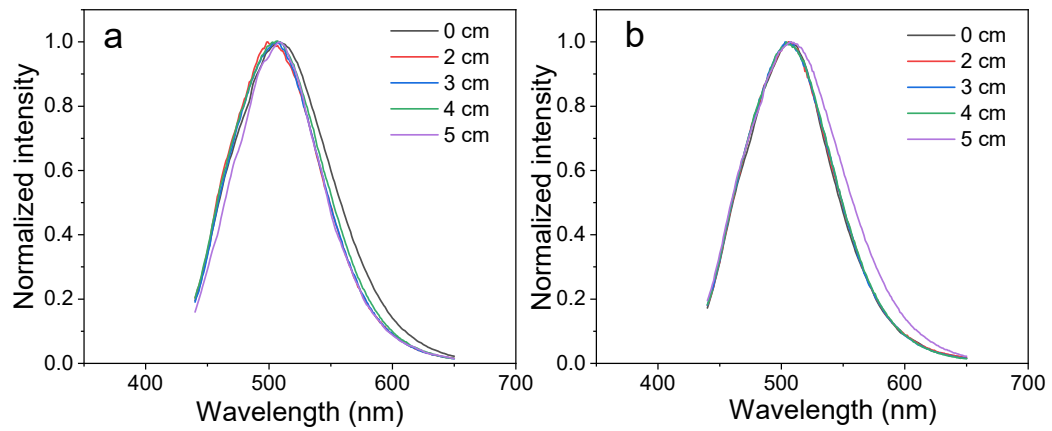


Fig S10 PL spectra measured at different optical paths for thin film LSCs: (a) Cdots based LSC, (b) Cdots with Ag@SiO₂ based LSC, PL₀ was peak emission intensity at optical path of 0 cm and PL was peak emission intensity at different optical path

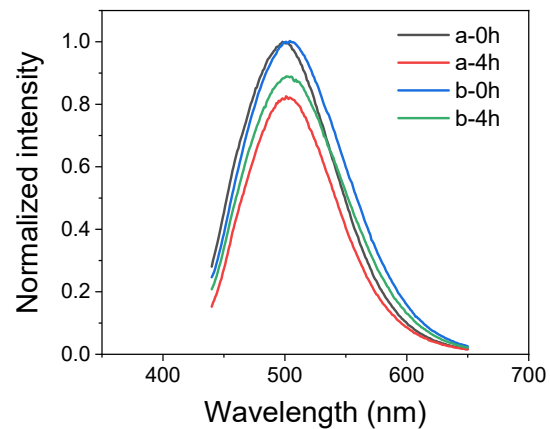


Fig S11 Photostability of thin film LSCs: (a) Cdots with Ag40@SiO₂, (b) bare Cdots. Normalization by PL₀ (initial peak emission intensity) and PL (peak emission intensity after 4 h UV radiation). Photostability was obtained by comparing the emission integral area

Reference:

1. C. Yang, D. Liu and R. R. Lunt, *Joule*, 2019, **3**, 2871-2876.
2. S. Chandra, J. Doran, S. J. McCormack, M. Kennedy and A. J. Chatten, *Sol. Energy Mater. Sol. Cells*, 2012, **98**, 385-390.
3. S. Chandra, J. Doran and S. J. McCormack, *Proceedings of International Conference CISBAT 2015 Future Buildings and Districts Sustainability from Nano to Urban Scale*, 2015, CONF. LESO-PB, EPFL, , 3-8.
4. C. Segura, V. Vargas, R. A. Valenzuela-Fernández, C. S. Danna and I. O. Osorio-Román, *ACS Appl. Energy Mater.*, 2020, **3**, 7680-7688.
5. A. Sethi, S. Chandra, H. Ahmed and S. McCormack, *Sol. Energy Mater. Sol. Cells*, 2019, **203**, 110150.
6. H. Y. Huang, K. B. Cai, Y. R. Sie, K. Li, J. M. Yeh and C. T. Yuan, *Solar RRL*, 2019, **3**, 1800347.
7. F. Mateen, H. Oh, W. Jung, M. Binns and S.-K. Hong, *Sol. Energy*, 2017, **155**, 934-941.
8. W. Zhou, Z. Q. He and X. J. Zhao, *Key Eng. Mater.*, 2014, **599**, 291-297.